ON THE VALIDITY OF MINER'S RULE UNDER LINEARLY COMBINED LOADING OF ROTATING BENDING AND CYCLIC TORSION

Shoji Harada

Dept. Mech. Engng, Faculty of Engng,
Kyushu Institute of Technology
Tobata, Kitakyushu 804 J A P A N

and

Tatsuo Endo

Dept. Mech. Engng, Faculty of Engng,
Kyushu Sangyo University, 2-3-1Matsukadai,
Higashi-ku, Fukuoka 813 J A P A N

1. INTRODUCTION

Fatigue life prediction under variable stress or strain amplitude is of importance in engineering practice. In this respect, various types of fatigue tests such as two-step, multi-step, block and random loading tests have been conducted. In almost all of those tests, although the stress amplitude and the mean stress are changed in the course of the fatigue tests, no change of the direction of principal stress axis occurs during the entire fatigue life. This means that the cumulative fatigue damage is caused by the coaxial load. On the contrary, some structural members are subjected to a combination load of cyclic bending and torsion. In such a case, the direction of principal stress or maximum shear stress axis varies during stressing. Therefore, the fatigue life prediction or cumulative fatigue damage induced by a combination of different type of stressing is of interest from a viewpoint of academic interest as well as engineering practice.

Few studies on the problem related have been seen in the literature. Within the scope of high cycle fatigue, the following problems have been discussed: (a) Fatigue limit in the case of combined loading of rotating bending(RB) and cyclic torsion(CY), and (b) Change of fatigue limit or fatigue life of the second stress cycle when the first stress reversals of RB or CY are cycled to a certain number, then switched to the second stress cycle. The

present study deals with the problem (b).

Concerning the problem (b), the following points have been investigated(1)-(7) so far: (1) The change of the fatigue limit of the second stressing when the over- or under- stressing by RB or CY is switched to the second stress cycling in the course of the fatigue life. (2) Cumulative fatigue damage in combination loading of RB and CY. Regarding to the point(2), some quantitative explanation has already been obtained. From the results(3)-(6), the loading type of RB-to-CY switching strengthens the fatigue life of the second stress cycle, while the fatigue damage is accumulated linearly in the case of CT-to-RB loading. The main objective of this study is to examine this load sequence effect on the fatigue damage accumulation through microscopic observation of the fatigue process. The fracture mechanics-aided approach is also applied to interpret that trend of the cumulative fatigue damage on the basis of the microcrack growth behaviour.

2. MATERIAL AND EXPERIMENTAL PROCEDURES

The material used is a medium carbon steel round bar(S45C,diameter 22mm). The chemical composition and the static tensile properties of the material are tabulated in Table 1 and Table 2 respectively. Figure 1 shows a geometry of hour-glass-shaped specimen used in both rotating bending and torsional fatigue tests. The stress concentration factors of the specimen are 1.011 for bending and 1.007 for torsion respectively. All the specimens were finished with a emery sand paper(#06) after machining, then annealed at 650°C for 30min and finally electropolished. A Vicker's indentation was introduced as a marking spot on the specimen surface to perform continual observation of the fatigue process. The rotating bending and torsional fatigue tests were conducted at a speed of 3400cpm and 2000cpm respectively. The observation of the microscopic fatigue process was done by a replication technique.

In examining cumulative fatigue damage by a combination loading of RB and CT, it should be noted that the reversals of cyclic bending stress amplitude σ by RB and cyclic torsional stress amplitude τ bring difference in fatigue damage even if the values of σ and τ are identical. Therefore, a condition of equivalence of fatigue damage by RB and CT should first be defined. In this respect, there is still no definite idea at this moment. Nisitani and Murakami(8) previously reported that if the cyclic maximum shear stress is same in fatigue by RB and CT, fatigue damage at the fatigue limit of crack initiation is similar in both types of loading. Taking this experimental evidence into account, the fatigue tests were mainly conducted for $\sigma/\tau=2$. Additionally, the fatigue tests were also conducted for $\sigma/\tau=\sqrt{3}, 1.58$.

3. EXPERIMENTAL RESULTS

3.1 CUMULATIVE FATIGUE DAMAGE BY COMBINATION LOADING OF RB AND CT

Figure 2 indicates S-N curves of the fatigue by RB and CT. From these S-N curves, the test condition for combination loading of RB and CT was determined as σ=250MPa and τ=125MPa. In counting cumulative fatigue damage, the scatter of the fatigue life at a definite stress level should be considered. To clarify this point the fatigue life at the prescribed stress level was examined using four specimens in each RB and CT type of loading. The results are expressed by the relationship between cumulative failure probability and number of stress cycles to failure, as illustrated in Figure 3. From these results, the mean fatigue life at the prescribed stress level was determined at a cumulative failure probability of 50%.

The combination loading by RB and CT was done as follows. When the first stress cycling by RB was repeated up to 20%, 40%, 60%, 80% of the mean fatigue life, then the stressing was switched to CT type of loading. In the case of CT-to-RB type of loading, the same procedure was employed. Figure 4 shows the results of the cumulative fatigue damage by the first and second stress cycles. A solid line in the figure denotes the case in which the Miner rule holds. All the results for σ/τ=2, $\sqrt{3}$, 1.58 are shown in the figure. Irrespective of the value of σ/τ, it is noted as a general trend that the Miner rule holds in the loading type of CT-to-RB switching, while first stress cycling strengthens the fatigue life of the second stress cycles in RB-to-CT switching. This trend is intensified for σ/τ=2, where the cyclic stress amplitude T is rather low as compared with other cases. For $\sigma/\tau=\sqrt{3}$, 1.58, it seems that the fatigue damages by the first and second stress cycles are uncoupled. The load sequence dependency of the cumulative fatigue damage can be understood as being induced by the difference in microscopic fatigue process in both types of loading combination. The detailed discussion on this point is described in the next paragraph.

3.2 CONTINUAL OBSERVATION OF THE MICROSCOPIC FATIGUE PROCESS

Difference in basic fatigue mechanism in RB and CT is first remarked before describing the results of the continual observation of the fatigue process. It is well known that the primary fatigue process of a low or medium carbon steel is dominated by the following process: First slip bands are formed in the ferrite grains at an early stage of the fatigue life. With

further increase of stress cycles, they grow up to slip band cracking and finally become microcracks. The direction of the slip band formation macroscopically coincides with the direction of the maximum shear stress. Figure 5 schematically illustrates the difference in slip band formation of a round bar specimen under RB and CT type of loading. In the case of RB type of loading, the maximum shear stress plane forms a conical plane. Therefore, the direction of slip band formation differs depending on the intersecting angle between the conical plane and the specimen surface, as shown in Figure 5(a). On the other hand, the slip bands are initiated in the direction either axial or circumferential direction of the specimen in the case of CT type of loading, as shown in Figure 5(b).

The continual observation of the fatigue damage from slip band formation to final failure was done for $\sigma/\tau=2$ and a condition of load switching of $n_1/N_1=0.4$. Figure 6 shows the result of the continual observation for σ-τ(RB-to-CT) type of loading. In this case, the slip band formation reveals a characteristic feature that the fatigue damages by RB band CT are uncoupled. It means that the slip band by the second stress cycles is formed at a position(see an arrow mark A in Figure 6(d)) different from a position(see an arrow mark A in Figure 6(d)) where the slip band is initially formed by the first stress cycles). Observing carefully the sequential photos, it is judged that the slip band growth during CT type of loading is rather restricted by the slip band previously formed by RB. Figure 7 depicts the microscopic monograph of a leading crack in RB-to-CT type of loading. The microcrack formed by slip band cracking is initially propagated in the direction of the maximum shear stress. Then, it is bifurcated and changed the propagation path to the direction of the principal stress axis 45°-inclined to the specimen axis. Figure 8 shows the growth of a leading crack observed in simple or pure CT type of loading. Comparing the morphologies of the formation and growth of the leading microcrack, it is seen that no discernible difference of microscopic fatigue process is noted between RB-to-CT and simple CT type of loading.

On the contrary, the fatigue damage is linearly cumulated in the case of CT-RB type of loading. Figure 9 indicates the results of the continual observation of the fatigue process. Although the slip bands are formed in both axial and circumferential direction of the specimen, the growth of slip bands originated in the circumferential direction(see an arrow mark D in Figure 9(b)) were dominant after switching of the loading type to RB. The microcrack was propagated macroscopically perpendicular to the axial direction without changing the propagation path. From these results, it is understood that the difference in the fatigue process between RB-to-CT and CT-to-RB type

of loading supports the difference of the macroscopic trend of the cumulative fatigue damage as shown in the Figure 4.

3.3 INTERPRETATION OF THE CUMULATIVE FATIGUE DAMAGE TREND ON THE BASIS OF THE MICROCRACK GROWTH

In order to examine the cumulative fatigue damage from a viewpoint of fracture mechanics the growth behaviour of a leading crack was traced from a grain-sized microcrack of about 20μm to a macrocrack of about 2-3mm just before final rapid growth by the replication method. Relationship between the crack growth rate dl/dN and the cyclic stress intensity factor range ΔK under simple loading, i.e., pure RB and CT, was evaluated using two specimens subjected to different level of cyclic stress amplitude. Figure 10 shows the result of the relationship between the crack growth rate dl/dN and the cyclic stress intensity factor range ΔK under single RB type of loading. The results in the case of simple CT type of loading is also shown in Figure 11. In both cases, the values of dK are calculated using a simple formula $\Delta K = \Delta\sigma\sqrt{\pi l/2}$ or $\Delta K = \Delta\sigma\sqrt{\pi l/2}$ where $\Delta\sigma$ and $\Delta\tau$ denote the full range of the cyclic stress amplitude in RB and CT respectively. The arrow marks in the Figure 11 indicate a change of the crack propagation mode from initial mode II to usual mode I. Even in the case of the simple CT type of loading, the main crack initiated at an early stage of the fatigue life changes its propagation path from mode II to mode I in the course of the fatigue process, as is seen in the Figure 8. In this respect, although the growth characteristic of the mode I and mode II crack should be separately treated as to evaluate rigorously the crack growth rate under pure shear, the mode II crack growth rate was estimated in the same manner as that in the mode I crack. From two figures, it is noted that the crack growth rate in simple RB implies considerably a linear trend for ΔK with less scatter, while dl/dN - ΔK relation shows some amount of scatter in simple CT. For comparison, the result of the simple RT is illustrated by a broken line in the Figure 11. It is observed in the Figure 11 that the crack growth rate in simple CT is first decelerated as compared with that in simple RB, then it quickly approaches the crack growth rate in simple RB after transition of the crack propagation mode from mode II to mode I.

Figures 12 and 13 show the relationship between dl/dN and ΔK in combination loading of RB-to-CT and CT-to-RB type respectively. The results in simple RB and CT type of loading are also shown by a broken line in each figure. The solid lines in both figures denote the average of dl/dN versus ΔK relationship determined by linear regression. In the case of RB-to-CT

switching, the leading crack initiated after load switching dominated the fatigue process, as previously described in the paragraph 3.2. The leading crack indicated transition of the crack growth mode from mode II to mode I(see arrow marks in the figure), as in the case of simple CT type of loading. The crack growth rate in this case is rather retarded as compared with that in simple CT type of loading. The reason for this crack retardation is understood as being induced by the hindrance of the slip bands formed during first stress cycles to the growth of the main crack initiated during second stress cycles. Whilst, in the case of CT-to-RB type of loading, the growth rate of the main crack shows rather small amount of scatter and coincides with the crack growth rate in simple RB type of loading. This tendency agrees with the effect of linear coupling of the cumulative fatigue damage, as mentioned in the paragraph 3.2. The discontinuity of the data observed in the Figure 13 is attributed to the fact that the value of dK becomes twice after switching of load.

4. DISCUSSION

The present result that the cumulative fatigue damage by RB and CT shows the effect of load sequence coincides with the results of other report(5)-(7). In this respect, few publications have been seen in the literature. To clarify the problem related the following points should be discussed.

(1) Equivalence of stress condition in counting cumulative fatigue damage when subjected to combination loading of different type
(2) Interpretation of the result on the basis of statistical viewpoint
(3) Quantitative evaluation and fracture-mechanics-aided consideration on the cumulative fatigue damage

Concerning the factor(1), the main portion of the present study was conducted under the condition of $\sigma = 2\tau$, i.e, equivalence of maximum shear stress. According to the result by Nisitani and Murakami(8), that condition represents the condition to ensure coincidence of the initiation life of persistent slip band(PSB) or grain-sized microcrack under RB or CT. However, it is easily suggested that even the slip band cracking initiates at the same life in RB and CT, subsequent crack growth obviously differs because of the difference of the stress condition on the maximum shear stress plane. That is, normal stress component of the value of half of the cyclic stress amplitude acts on that plane in RB, while the normal stress component acting on that plane is zero in CT. Therefore, in counting cumulative fatigue damage under application of different type of stressing, some criterion which also ensures the equivalence of stress condition during microcrack growth period.

Considering the present results from this standpoint, it is noted that although the trend of the cumulative fatigue damage in RB-to-CT type of loading is generally same irrespective of the value of σ/τ, slight difference of the trend which varies depending on σ/τ is observed in the Figure 4. In the case of $\sigma/\tau=2$, the value of n_1/N_1 falls between 1.0 and 1.6. On the contrary, those values gather near 1.0 in the case of $\sigma/\tau=1.58$, 3. This difference can be understood as being induced by the difference of the hindrance effect of the first-stress-cycles-formed slip bands to the growth of the microcrack during the second stress cycles. For the higher value of σ/τ, the torsional stress amplitude is low enough to develop strengthening of the microstructure by slip and to retard the initiation and propagation of the microcrack, whilst τ is high enough to initiate and propagate microcrack by own second stress cycles. Stress level dependency of the hindrance effect will be discussed in further study.

Regarding to the factor(2), the scatter of the data is generally attributed to two factors; scatter caused by material itself and the scatter caused by experimental accuracy. Concerning the latter factor, it should be noticed that in CT-to-RB type of loading, misalignment-induced initial bending in setting up specimen results in cyclic creep during RB type of loading. As the result, a large amount of scatter or error is involved in the data. In this study, special attention is paid to minimize the initial bending strain less than 10×10^{-6}. The fatigue damage is usually evaluated by $\Sigma(ni/Ni)$, where the average value of Ni is taken as a standard life at a prescribed stress level. A reliability-based Miner's rule(9) $E(\Sigma(ni/Ni))=1$ should be brought to discuss the problem related when the applicability of Miner's rule of each specimen is considered. In order to get statistical interpretation on the microcrack-fatigue-process-oriented cumulative fatigue damage, extensive studies are needed.

Considering the factor(3), the fracture-mechanic-aided approach is suggested fundamentally possible and useful to examine quantitatively the cumulative fatigue damage problem in combination loading of different type of stressing. In this regard, a microcrack growth law-aided approach, in current prevalent, is indispensable in investigating the problem related. In particular, the criterion of the crack growth mode transition from mode II to mode I as observed in RB-to-CT and simple CT type of loading should be established. Furthermore, difference of the crack growth rate between mode I and mode II should be studied as to make understanding of the problem of the cumulative fatigue damage. Additionally, the hindrance effect of the first stress- cycles-formed slip bands to the microcrack growth during second stress cycles, as mentioned so far, should further be studied. It is well known that

pre-fatigue damage or stress or strain cycle history has no influence on the subsequent mode I crack growth in high cycle fatigue. This evidence is also experimentally clarified in low cycle fatigue regime(10). Therefore, the hindrance effect which enhances the fatigue strength becomes significant just after switching of load and initial period of microcrack initiation and propagation during second stress cycles in RB-to-CT type of loading. As far as the stress level dependency of the trend of the cumulative fatigue damage in RB-to-CT type of loading is concerned, that effect should be further examined.

Finally, it is noted that anisotropy of material is a relating factor in discussing the problem related. Microcracks generally initiate in a statistical manner equally in both axial and circumferential direction of the specimen under torsional fatigue. However, in the present study, all the leading cracks were formed from the slip band cracking initiated in the circumferential direction. This might be caused by the effect of rolling-inducedmechanical fibering or texture ofthe specimen microstructure(11). Although the microcrack initiated at an early stage of the fatigue life changed its propagation mode from mode II to mode I in the course of the fatigue process, irrespective of the loading mode and combination condition, it can be suggested that the microcrack growth was strongly affected by the microstructure, especially anisotropy of the microstructure, during initial and transient process of the crack growth.

5. CONCLUSIONS

Cumulative fatigue damage by combination loading of rotating bending(RB) and cyclic torsion(CT) is investigated on a medium carbon steel in high cycle fatigue regime. To examine the effect of load sequence two types of combination loading,i.e., RB-to-CT switching and CT-to-RB switching of load, are employed. Stress condition for combination loading is varied as $\sigma/\tau = 2, \sqrt{3}, 1.58$. The trend of the cumulative fatigue damage is examined through continual observation of the fatigue process. In order to have some quantitative understanding on the problem related fracture-mechanics-aided approach is also applied to evaluate the microcrack growth rate. The results obtained are briefly summarized as follows.

(1) The first stress cycles microscopically have a strengthening effect on the subsequent second stress cycles in the case of RB-to-CT type of loading. This trend slightly differed depending on the value of σ/τ. For the higher value of σ/τ, the strengthening effect is significant, while the fatigue damage is rather uncoupled for the lower value of σ/τ. On the contrary, the fatigue

damage is linearly cumulated in the case of CT-to-RB type of loading, irrespective of the value of σ/τ. The Miner rule is applied in that case.

(2) In the case of RB-to-CT loading mode, the growth of slip band cracking,being formed during second stress cycles irrespective of the first stress cycles, dominated the fatigue process. The significant strengthening effect at $\sigma/\tau=2$ can be suggested to be caused by the hindrance effect of the first-stress-cycles-formed slip bands to the growth of the microcrack during second stress cycles.

(3) The microcrack initiated during first stress cycles was propagated in a coaxial direction after switching of loading mode in the case of CT-to-RB type of loading. This behaviour of microcrack growth well supports the macroscopic tendency of the linear cumulative fatigue damage.

(4) The fracture-mechanics-aided evaluation of the microcrack growth behaviour in simple and combination loading mode was found useful to understand the macroscopic and microscopic trend of the cumulative fatigue damage under combination loading mode.

ACKNOWLEDGMENT

The authors wish to acknowledge the assistance of Mr. Yasuhiko Shimizu, presently an engineer at Toshiba Electric Company Ltd., in carrying out the experiment.

REFERENCES

(1) Nishihara, T., and Kawamoto, M., Trans. Japan Soc. Mech. Engrs., Vol.9(1943), No.35, p.37.
(2) Kitaoka, S., et al., Trans. Japan Soc. Mech. Engrs., Vol.35, No.280(1969), p.2293.
(3) Nakamura, H., et al., Trans. Japan Soc. Mech. Engrs., Vol.35, No.278(1969), p.2012.
(4) Nakamura, H., et al., Trans. Japan Soc. Mech. Engrs., Vol.36, No.292(1970), p.1969.
(5) Katoh, Y., et al., Technology Reports of the Gifu University., No.19(1969), p.27.
(6) Ando , Y., et al., J. Soc. Materi. Sci. Japan., Vol.23, No.252(1974), p.765.
(7) Ohji, K., et al.,Preprint. Japan Soc. Mech. Engrs., No.734-2(1973), p.7.
(8) Nisitani, H., and Murakami, Y., Trans. Japan Soc. Mech. Engrs., Vol.35, No.275(1969), p.1389.
(9) Ichikawa, M., J. Japan Soc. Precision Engineering., Vol.50, No.10(1984), p.1550.
(10) Harada, S., ASTM STP942., (1988), p.1181.
(11) Harada, S., et al.,Trans. Japan Soc. Mech. Engrs., Vol.53, No.485(1987), p.26.

Table 1 Chemical composition of the material tested (wt %)

C	Si	Mn	P	S	Cu	Ni	Cr
0.24	0.28	0.42	0.013	0.015	0.01	0.01	0.02

Table 2 Mechanical properties of the material tested

σ_{sl} (MPa)	σ_B (MPa)	φ (%)	ψ (%)
268	442	35.8	57.6

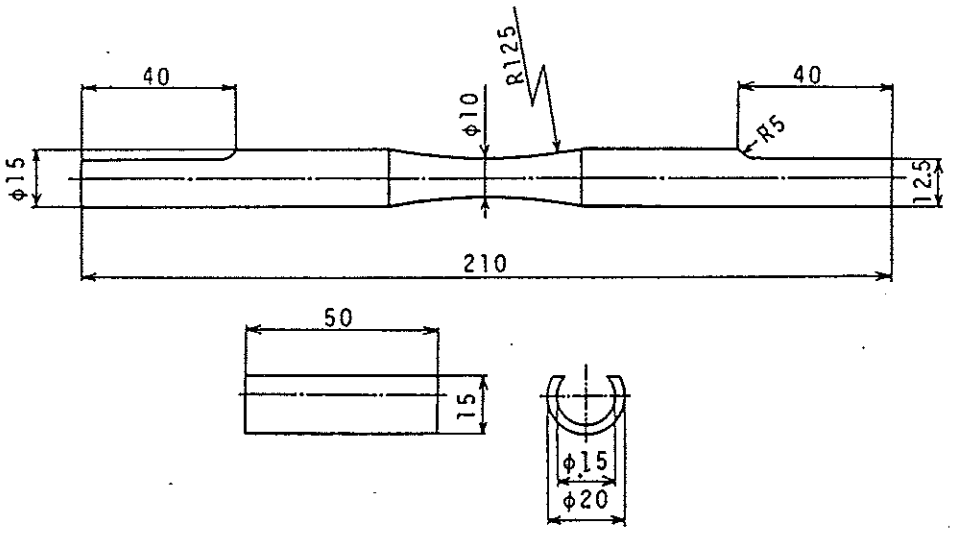

Fig. 1 Geometry of the specimen tested for RB and CT type of loading

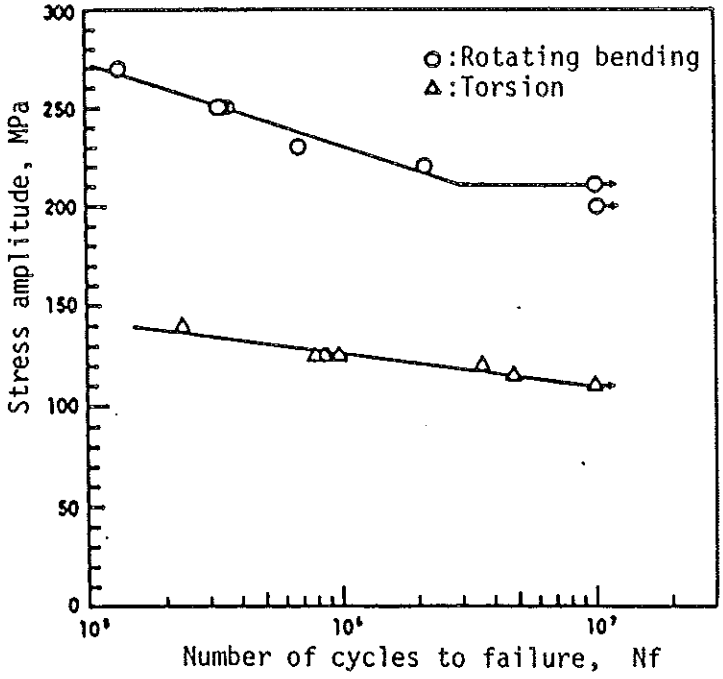

Fig. 2 S-N curves in RB and CT type of loading

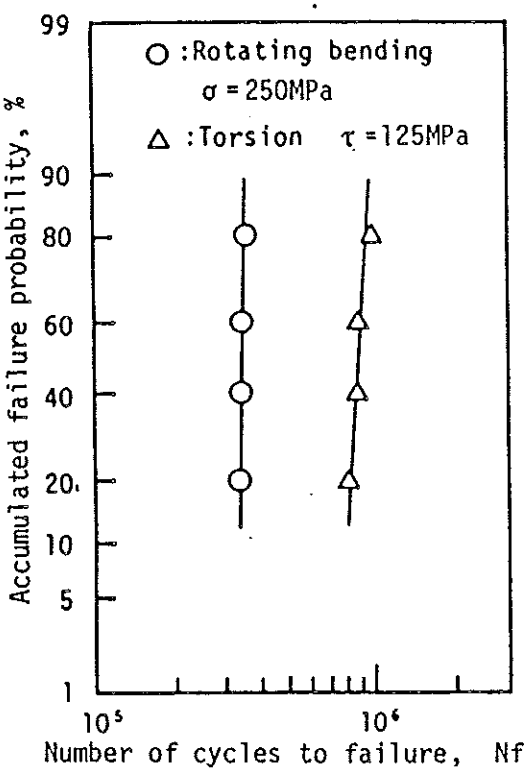

Fig. 3 Cumulative failure Probability in RB and CT fatigue

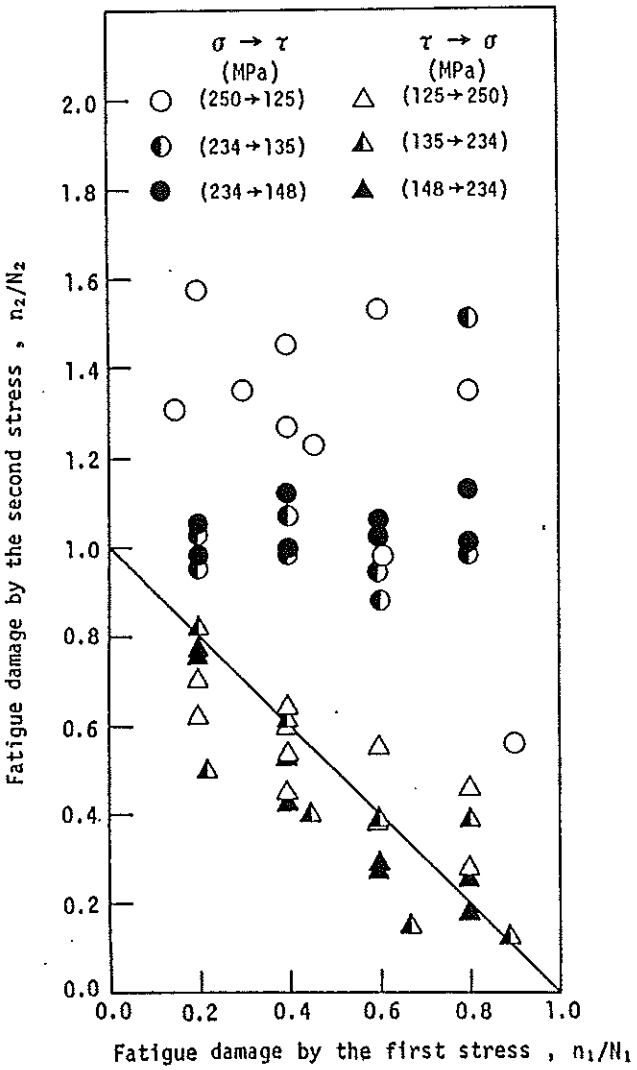

Fig. 4 Cumulative fatigue damage in RB-to-CT and CT-to-RB type of combination loading

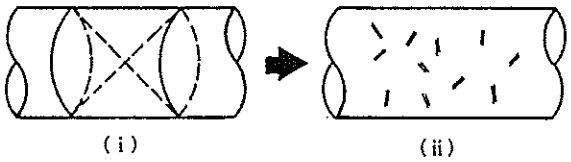

(a) Simple RB fatigue

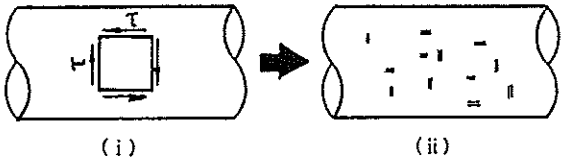

(b) Simple CT fatigue

Fig. 5 Schematical illustrations of slip band formation in simple RB and CT fatigue

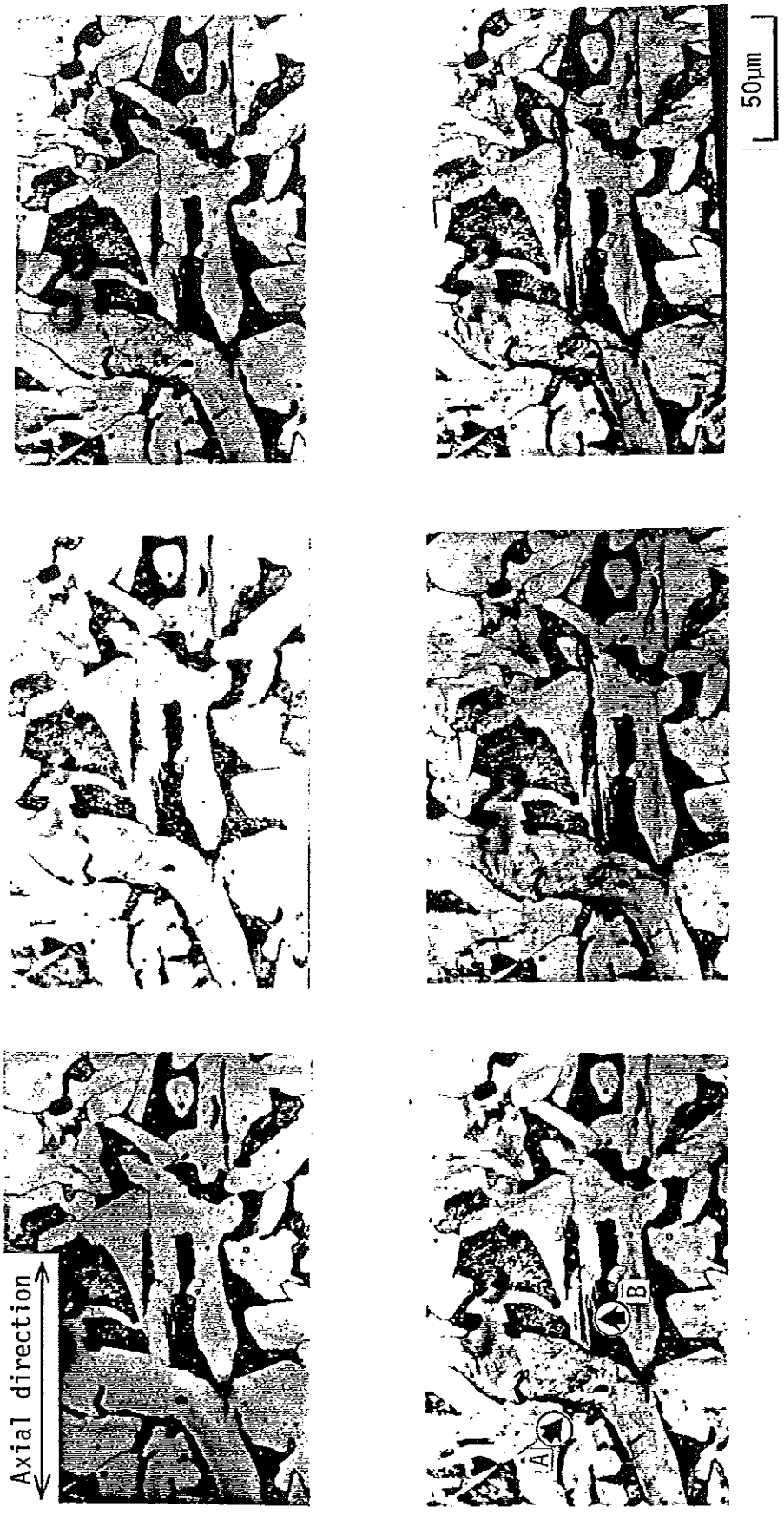

Fig. 6 Continual observation of the fatigue process in RB-to-CT type of loading

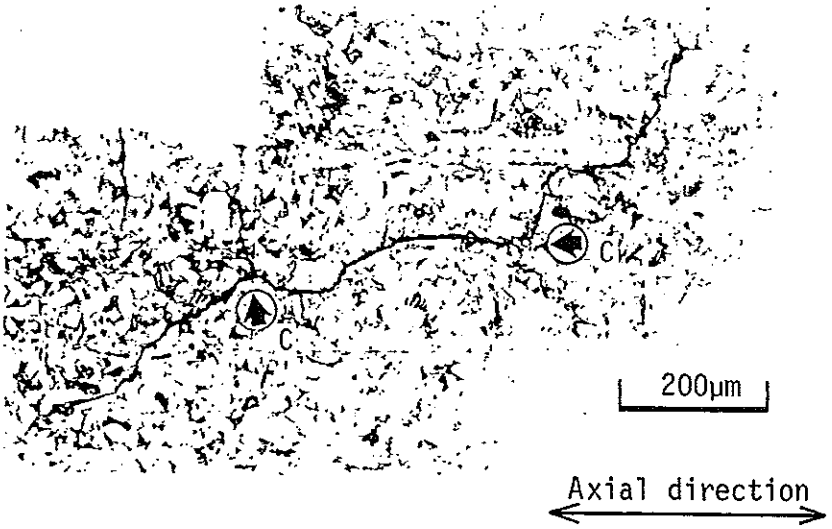

Fig. 7 Growth and bifurcation of a leading crack in RB-toCT type of loading

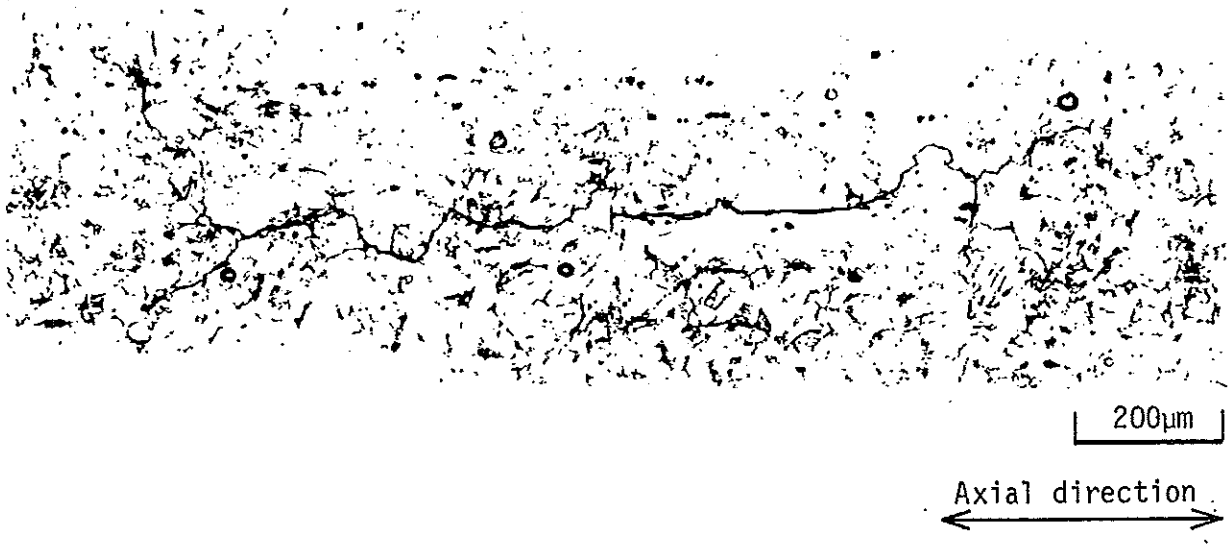

Fig. 8 Crack growth morphology in simple CT fatigue

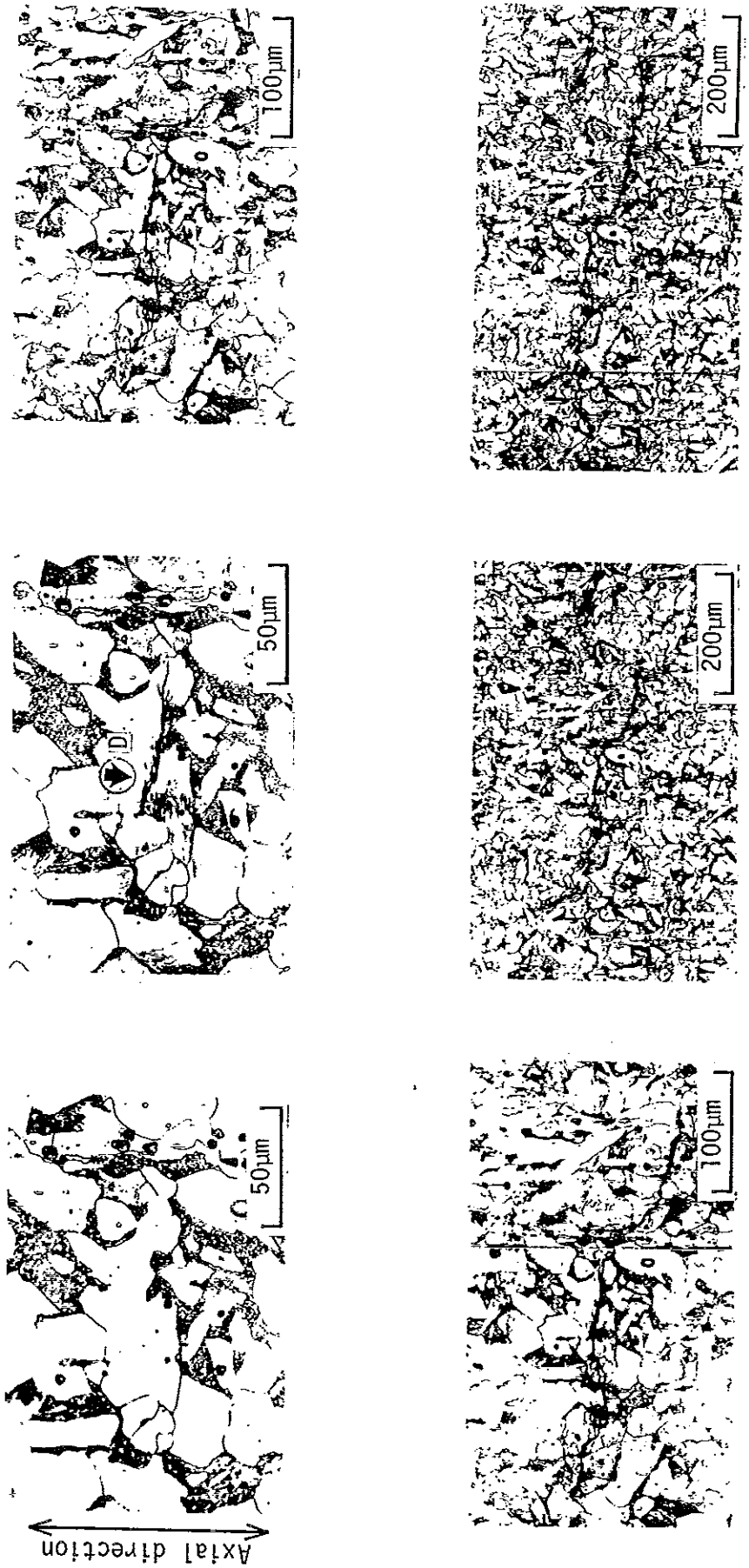

Fig. 9 Continual observation of the fatigue process in CT-to-RB type of loading

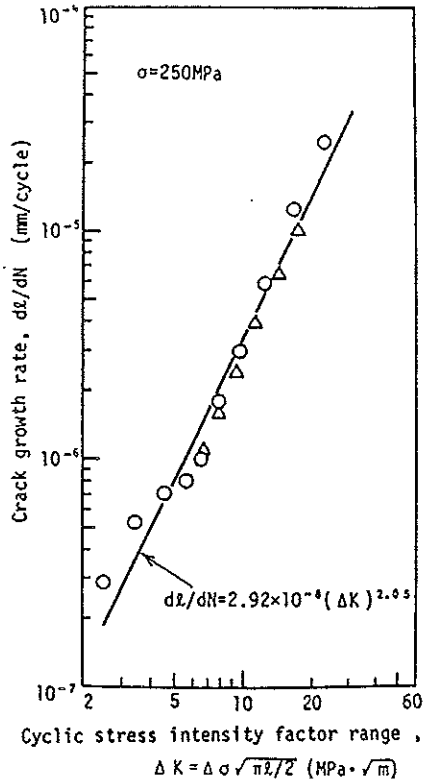

Fig. 10 Crack growth rate curve in Simple RB fatigue

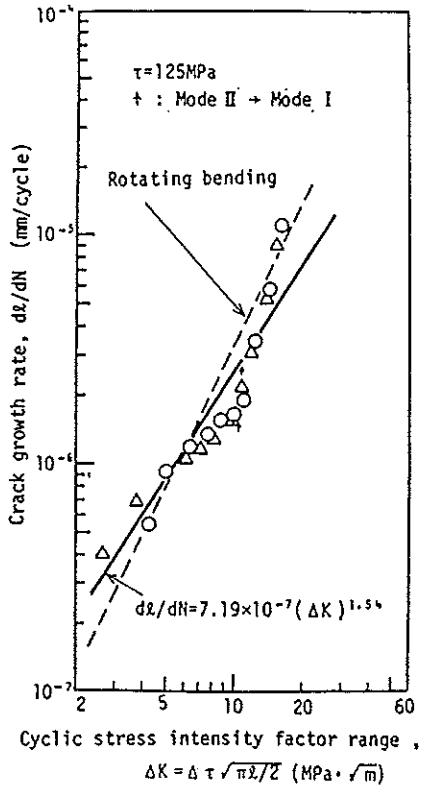

Fig. 11 Crack growth rate curve in simple CT fatigue

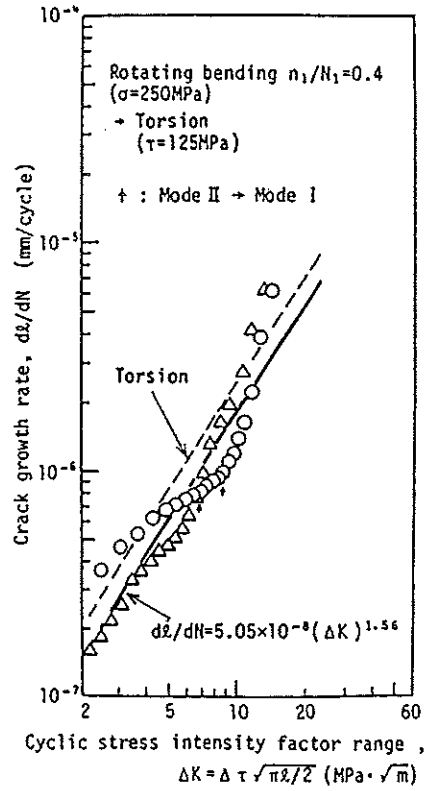

Fig. 12 Crack growth rate curve in combination loading of RB-to-CT type

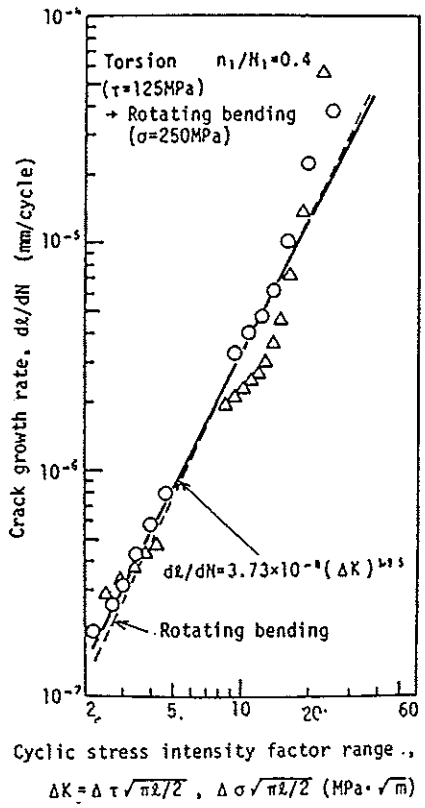

Fig. 13 Crack growth rate curve in combination loading of CT-to-RB type